Journal of
Applied Physics

Effect of a thin (doped) PZT interfacial layer on the properties of epitaxial PMN-PT films

Cite as: J. Appl. Phys. **128**, 055302 (2020); https://doi.org/10.1063/5.0004479
Submitted: 26 February 2020 . Accepted: 15 July 2020 . Published Online: 03 August 2020

Muhammad Boota, Evert P. Houwman, Giulia Lanzara, and Guus Rijnders

ARTICLES YOU MAY BE INTERESTED IN

Wurtzite quantum well structures under high pressure
Journal of Applied Physics **128**, 050901 (2020); https://doi.org/10.1063/5.0004919

Growth of bulk GaN crystals
Journal of Applied Physics **128**, 050902 (2020); https://doi.org/10.1063/5.0009900

Stability of ferroelectric and antiferroelectric hafnium-zirconium oxide thin films
Journal of Applied Physics **128**, 054101 (2020); https://doi.org/10.1063/5.0011547

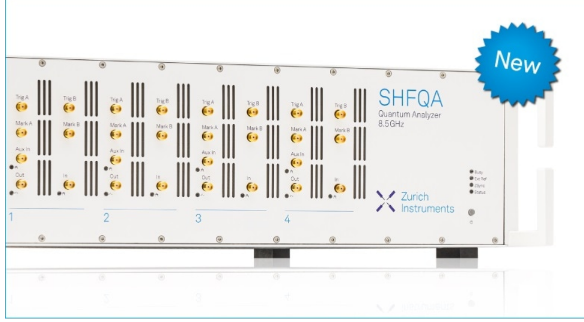

© 2020 Author(s).

Journal of Applied Physics ARTICLE scitation.org/journal/jap

Effect of a thin (doped) PZT interfacial layer on the properties of epitaxial PMN-PT films

Cite as: J. Appl. Phys. **128**, 055302 (2020); doi: 10.1063/5.0004479
Submitted: 26 February 2020 · Accepted: 15 July 2020 ·
Published Online: 3 August 2020

Muhammad Boota,[1,2,a)] Evert P. Houwman,[1,b)] Giulia Lanzara,[2] and Guus Rijnders[1]

AFFILIATIONS

[1]MESA+ Institute for Nanotechnology, Faculty of Science and Technology, University of Twente, P.O. Box 217, 7500AE Enschede, The Netherlands
[2]Engineering Department, University of Rome "ROMA TRE," Via della Vasca Navale 79, 00146 Rome, Italy

[a)]**Present address:** Department of Physics, University of Lahore, Raiwand Road, Sultan Town, Lahore, Pakistan.
[b)]**Author to whom correspondence should be addressed:** e.p.houwman@utwente.nl

ABSTRACT

Pure perovskite phase, (001)-oriented, epitaxial thin films of $(Pb(Mg_{1/3}Nb_{2/3})O_3)_{0.67}$-$(PbTiO_3)_{0.33}$ (PMN-PT) were fabricated on single crystal, (001)-oriented $SrTiO_3$ substrates using a hard (Fe-doped) and soft doped (Nb-doped) PZT(52/48) interfacial layer. The effect of different interface layers on the structural and ferroelectric properties of the PMN-PT films was investigated in detail. A significant self-bias voltage in the PMN-PT films can be introduced by using an appropriate interfacial layer. There are significant differences in polarization for different types of doped and undoped interface layers and a doubling of the relative dielectric constant was observed for the Nb-doped interfacial layer. Device properties remain stable up to at least 10^8 cycles.

© 2020 Author(s). All article content, except where otherwise noted, is licensed under a Creative Commons Attribution (CC BY) license (http://creativecommons.org/licenses/by/4.0/). https://doi.org/10.1063/5.0004479

I. INTRODUCTION

$(Pb(Mg_{1/3}Nb_{2/3})O_3)_{0.67}$-$(PbTiO_3)_{0.33}$ [PMN-PT(67/33) or short PMN-PT] is a material of great interest for the fabrication of hyperactive piezo-MEMS for the purpose of sensing and actuation.[1] The superior piezo-response ($d_{33} \approx 2500$ pm/V, $e_{31} = -27$ C/m^2) demonstrated by this PMN-PT compared to the well-known and much investigated material $PbZr_{0.52}Ti_{0.48}O_3$ (PZT) has propelled it to the forefront of research and development.[1,2] The longitudinal piezoelectric coefficient (d_{33}) observed for a PMN-PT single crystal is an order of magnitude higher than that for PZT.[2] Likewise, the transverse piezoelectric coefficient (e_{31}) of epitaxial PMN-PT thin films in a freestanding cantilever configuration was found to be significantly higher than that of epitaxial PZT thin films.[1] In addition, the superior coupling coefficient ($k_{33} > 0.9$) along with low dielectric losses (<1%) could make this material an auspicious candidate for the fabrication of next generation piezo-MEMS sensors and actuators.[1,3] Piezo-MEMS devices fabricated from this material with its superior properties may generate large strains for a small applied field or vice versa be sensitive to very small strain.

Doping elements used for bulk and thin film PZT ceramics are typically categorized into hard doping and soft doping, which refer to increasing or decreasing the coercive field of the polarization hysteresis loop of these materials. Hard doping usually arises from acceptor doping, whereas soft doping is generally due to donor doping.[4] PZT is a perovskite material which crystal structure is described with the formula ABO_3. It consists of two types of positively charged ions, i.e., A^{2+} and B^{4+} (cations) and O^{2-} anions. Hard doping (or acceptor doping) refers to the situation in which some of the A-site atoms (A^{2+}) are replaced by monovalent dopant elements (X^{1+}) or some B-site atoms (B^{4+}) are replaced by trivalent dopant elements (X^{3+}). These situations are known as A-site and B-site acceptor doping, respectively. Similarly, soft doping refers to the situation in which some A-site atoms (A^{2+}) are replaced with trivalent dopant elements (X^{3+}) or the B-site atom (B^{4+}) is replaced with a penta-valent dopant element (X^{5+}). This situation is commonly identified as A-site and B-site donor doping, respectively.[5] In this study, $Pb(Zr_{0.52}Ti_{0.48})O_3$ doped (1.0 mol.%) with iron (Fe^{3+}) and niobium (Nb^{5+}) at the B-site, acting as acceptor and donor dopants, respectively, were selected as the interfacial layer between the $SrRuO_3$ base electrode and the PMN-PT thin film, in order to investigate the effect of doping on the properties of the PMN-PT film.

© Author(s) 2020

Haccart and co-workers performed a study on the effect of Nb concentration on the properties of PZT films deposited by sputtering on platinized silicon. They observed a relatively high self-bias for low Nb doping level (2 at. %) compared to high doping level (7 at. %).[7] Subsequent work performed by different groups shows the effect of Nb doping on the electrical properties (specifically of the self-bias) of textured PZT films, reporting an enhancement of ferroelectric and piezoelectric properties of the Nb-doped PZT films.[6,8,9]

The effect of the B-site acceptor dopant (Fe) concentration was studied by Majumder and co-workers who showed a decrease in remnant polarization with increasing acceptor dopant concentration.[10] Bai *et al.*[11] investigated the effect of Fe concentration on the properties of PZT thin films deposited by the sol-gel method. They observed a Fe concentration dependent shift of the ferroelectric loop, which was ascribed to a change in the oxygen vacancy density. Dawber and Scott reported that the mobile charged defects formed by oxygen vacancies can easily accumulate near the film/electrode interfaces due to the higher mobility of the oxygen vacancies than those of lead. This results in the formation of interfacial layers under an external field. These can result in a shift of the hysteresis loops.[12,13]

It is noticed here that most of the work reported on doped PZT films is on polycrystalline thin films and that the physical mechanisms behind the origin of different characteristics in acceptor and donor doped PZT films are not fully understood yet. Furthermore, the ferroelectric and piezoelectric properties of (doped) epitaxial thin films and the physical mechanisms arising from doping may be different from those in polycrystalline thin films.

A PZT interfacial layer is found to be very beneficial for the growth of perovskite pure phase PMN-PT thin films.[14] Such an interface layer was also found to broaden the process window for the growth of polycrystalline PMN-PT films.[15]

In this study, we have investigated the effect of hard (Fe) and soft (Nb) doped epitaxial $Pb(Zr_{0.52}Ti_{0.48})O_3$ interfacial layers on the properties of epitaxial PMN-PT (67/33) films on $SrTiO_3$ substrates. Doping concentrations of 1.0 mol.% Nb^{5+} as donor and 1.0 mol.% Fe^{3+} as acceptor on the B-site (Zr^{4+}/Ti^{4+} site) of PZT were selected based on the literature.[6,7,11] The results are compared with epitaxial PMN-PT (67/33) films, prepared without respectively with an un-doped PZT interfacial layer.

II. EXPERIMENTAL PROCEDURE

The PMN-PT/(un-)doped PZT (200 nm/25 nm) bilayer stack was sandwiched between 100 nm $SrRuO_3$ electrodes. The (doped) PZT layer is between the bottom electrode and the PMN-PT film. The complete hetero-structure was deposited on a 0.5 mm thick, (001) oriented $SrTiO_3$ substrate. The $SrTiO_3$ substrates were pretreated prior to deposition to achieve TiO_2 single termination using the method developed by Koster *et al.*[16] All films have been deposited by Pulsed Laser Deposition (PLD) using a KrF excimer laser operating at 248 nm. The PMN-PT films were deposited at a substrate temperature of 585 °C while keeping the oxygen pressure at 0.27 mbar at a laser fluency of 2.0 J/cm^2 and at 4 Hz repetition rate. The PZT films (doped and un-doped) were fabricated at a substrate temperature of 600 °C and an oxygen pressure of 0.10 mbar at a laser fluency of 3.5 J/cm^2 and at 2 Hz repetition rate. The substrate was placed at a distance of 6 cm from the target during PMN-PT and PZT depositions. The complete hetero-structure was deposited without breaking the vacuum to avoid unwanted contaminations. The layer stack was cooled down to room temperature immediately after deposition in a 1 bar oxygen ambient with a cooling rate of 10 °C/min. The specific growth conditions for $SrRuO_3$ are reported elsewhere.[17] The results for these films are compared with those of a 200 nm thick PMN-PT thin film capacitor deposited on an undoped PZT layer, respectively, directly on the SRO buffered STO substrate, deposited with nearly the same deposition conditions. The latter device structure (device S0) was discussed in a different context in Ref. 14.

Structural properties and the epitaxial relationships were investigated by HR-XRD (PANalytical X^{1}pert PRO MRD) and HR-SEM. The in-plane and out-of-plane lattice parameters were derived from reciprocal space maps. Ferroelectric capacitor devices ($200 \times 200\,\mu m^2$) were patterned by a standard photolithography process and structured by argon ion beam etching. Polarization–electric field (P–E) hysteresis loops were measured using a modified Sawyer Tower circuit (AixACCT TF Analyser 3000) at a frequency of 1 kHz using a bipolar triangular pulse with 150 kV/cm amplitude. Fatigue measurements were performed using a rectangular pulse train at a frequency of 10 kHz and an amplitude of 150 kV/cm. The longitudinal piezoelectric coefficients (d_{33eff}) were obtained using a polytec MSA-400 micro scanning laser doppler vibrometer. The capacitance vs electric field (C–E) measurements have been performed using a Suss MicroTech PM300 probe station equipped with a Keithley 4200 semiconductor characterization system at 10 kHz and an amplitude of 150 kV/cm. The corresponding dielectric constants have been calculated from these C–E curves.

III. RESULTS AND DISCUSSION

A. Crystalline structure

Figure 1(a) shows the θ–2θ diffraction patterns of the epitaxial PMN-PT films deposited on an iron and niobium doped PZT interfacial layer as well as on an un-doped PZT interfacial layer. The reflections corresponding to the substrate, the electrode, PMN-PT, SRO, and PZT layers are indicated [Fig. 1(b)]. The solid green lines are drawn to specify the reflection positions of the corresponding bulk materials. The diffractograms show the peaks corresponding to the (001) growth orientation of PMN-PT and PZT films only. No diffraction peaks due to impurity phases (pyrochlore phase) or other orientations were observed for both (PMN-PT, PZT) ferroelectric materials within the detection limits of our instrument.

Rocking curve measurements (log scale) are shown in the inset of Fig. 1(a). Full width at half maximum (FWHM) values of 0.06° to 0.11° for (002) rocking curves are even better than values reported for commercially available PMN-PT single crystals (FWHM = 0.14°),[1] demonstrating the high degree of oriented growth and excellent crystalline quality of the deposited epitaxial PMN-PT films. On the other hand, the FWHM of a PMN-PT film deposited directly on SRO/STO is 0.52° (not shown). This demonstrates the beneficial effect of a PZT

© Author(s) 2020

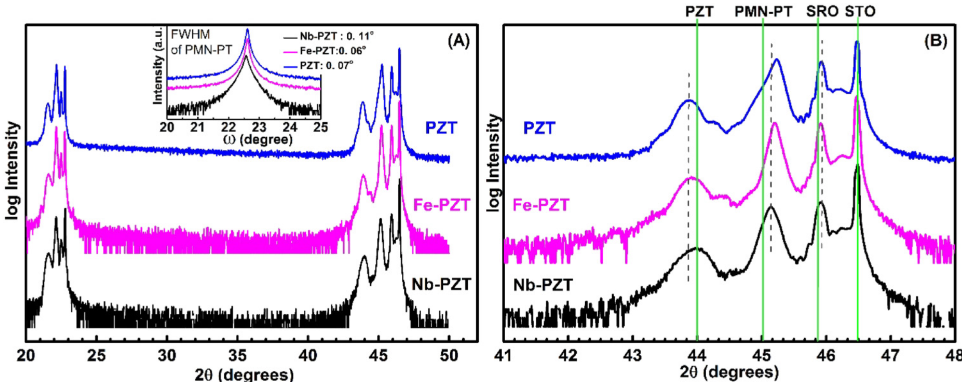

FIG. 1. (a) XRD pattern of epitaxial PMN-PT films deposited using Nb-doped, Fe-doped, and un-doped PZT interfacial layer on the STO substrate. The inset shows PMN-PT rocking curves for (001) reflections. (b) Zoom-in of the (002) diffraction peaks indicating the peak shift (variation in out-of-plane lattice constants) based on the nature of the interfacial layer material. Bulk peak positions are marked with solid green lines and peak shits are indicated by the dotted gray lines.

buffer layer for the growth of PMN-PT, providing a lattice match layer between the STO/SRO (a = 3.905 Å) and PMN-PT (a = 4.022 Å).

The PZT interfacial layer *θ–2θ* reflections are shifted from the expected angle for *c*-axis oriented unstrained PZT. The peak shift toward a lower angle indicates a change in the out-of-plane lattice constant. The reciprocal space map (RSM) of the (013) reflections of the film stacks (not shown) indicates that the SRO-bottom electrode is fully strained to the STO substrate, whereas the in-plane lattice parameters of the (un-)doped PZT and the PMN-PT layers are approximately equal but not strained to the substrate. This holds for all samples, see Table I, implying that the epitaxial lattice strain between the (doped) PZT and the strained SRO (with in-plane lattice constant equal to that of the STO substrate is 3.905 Å) is largely relaxed in the (un-)doped PZT within a very thin layer of at the most a few nanometers. The (doped) PZT (with MPB composition) adopts the tetragonal phase with the long crystal axis normal to the film plane. The unstrained shortest lattice constant of the PZT(MPB) composition in bulk is 4.035 Å and the long axis as 4.160 Å;[18] thus, the PZT interfacial layers appear very slightly tensile strained in the film plane.

From the measured lattice parameters, the unit cell volumes and the percentual change with respect to the bulk value are calculated (see Table I). The unit cell volume of the PZT layers is slightly reduced from the bulk value. Furthermore, the *c*/*a* ratio of the undoped and doped films is slightly smaller than the bulk value. We think that both features are due to a high density of incorporated defects to relax the substrate induced epitaxial strain in the thin layer adjacent to the bottom SRO electrode. Note that the measured in-plane lattice parameters of the (doped) PZT layers are equal within the error margins of the measurement (estimated as ±0.004 Å), indicating that doping does not influence the initial growth of these layers.

The measured in-plane lattice parameters of the PMN-PT-on-PZT layers are also equal (within ±0.004 Å) but slightly less than that of the underlying (doped) PZT layers and approaching the PMN-PT bulk lattice parameter. This indicates that also the

TABLE I. In-plane and out-of-plane lattice parameters of the PZT interfacial layers and the PMN-PT films deposited on SRO electroded STO substrates.

	Interfacial layer (PZT)				PMN-PT			
Sample	a (Å)[a]	c (Å)[a]	$\Delta V/V_{blk}$[b]	c/a	a (Å)	c (Å)	$\Delta V/V_{blk}$[b]	c/a
Bulk PMN-PT	4.035[c]	4.161[c]		1.031	4.022[d]	4.022[d]		1.000
No PZT seed layer					4.020	4.039	0.32%	1.005
Undoped PZT	4.042	4.130	−0.40%	1.022	4.028	4.007	−0.08%	0.995
Fe-PZT	4.042	4.124	−0.55%	1.020	4.028	4.008	−0.05%	0.995
Nb-PZT	4.037	4.123	−0.81%	1.021	4.025	4.013	−0.07%	0.997
Average[e]	4.039				4.027			

[a]Error ±0.004 Å.
[b]±0.29% maximum error due to error in *a*, *c*.
[c]Rossetti *et al.*[18]
[d]Pseudocubic parameters.
[e]Average of measured *a*-parameters of undoped, Fe- and Nb-doped PZT, and PMN-PT on these interfacial layers.

© Author(s) 2020

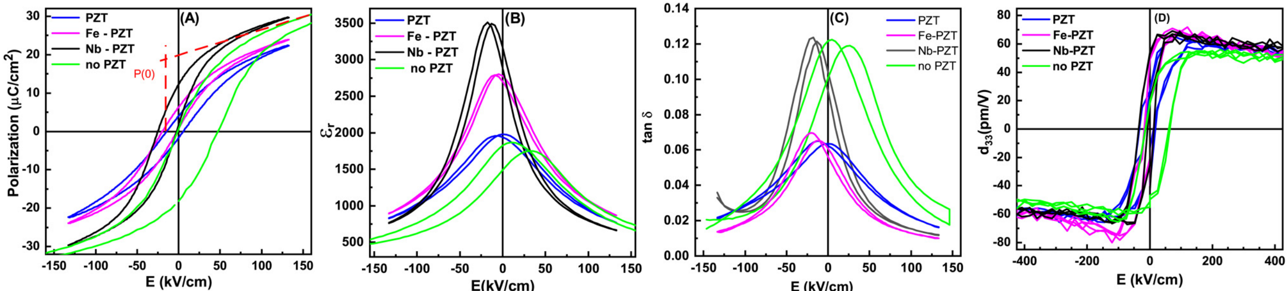

FIG. 2. (a) Polarization hysteresis loops; (b) relative dielectric constant; (c) loss tangent curves derived from the electric field vs capacitance measurements; and (d) the effective out-of-plane piezoelectric coefficient of 200 nm thick PMN-PT films deposited, respectively, on 25 nm of undoped PZT, 25 nm of 1% Fe-doped, 1% Nb-doped PZT, and directly on a 100 nm SRO bottom electrode on a single crystal, (001)-oriented STO substrate. All loops are measured before aging of the samples.

PMN-PT layers relax rapidly most of the small tensile strain imposed by the (doped) PZT layer. The in-plane lattice parameters of the PMN-PT layer directly on the SRO/STO is smaller than that of the layers on the (doped) PZT, reflecting that the significant imposed compressive strain of the SRO/STO affects the average strain in the PMN-PT. The PMN-PT unit cell volumes of the films on (doped) PZT are equal to the bulk value (within the measurement errors), as are the c/a ratios. The unit cell volume and c/a ratio of the PMN-PT directly grown on SRO/STO are slightly larger than of other films. We ascribe this difference to the different initial strain induced by the STO/SRO respectively (doped) PZT interfacial layer, causing a slightly different defect density. [However, it may also partly be due to the slightly different deposition conditions used for this film (this is the S0 sample in Ref. 14, knowing that the structural and electrical properties of PMN-PT thin films are very sensitive to the deposition conditions.[17]]

Cross-sectional SEM analysis (not shown) of PMN-PT thin films grown on, respectively, STO/SRO and STO/buffer layers, in which the buffer layer has a pseudo-cubic lattice parameter similar to that of PZT, shows that the PMN-PT film on SRO shows many voids and a non-columnar crystalline structure. Nonetheless, the growth orientation is (001) with an angular spread of only 0.52° and shows in-plane registry of the lattice with the substrate. The much smaller FWHM of the PMN-PT films grown on (doped) PZT indicates that the crystalline quality of these films is much better than those grown on SRO directly. The SEM analysis shows very dense, columnar films that formally should be qualified as to be of polycrystalline, textured nature. However, to distinguish the relative high crystalline quality of these films from that of films derived from chemical solution deposition, we use here the more usually applied (although somewhat sloppy) qualification of epitaxial growth for these PMN-PT films.

We conclude that the PMN-PT layers on the different (doped) PZT layers are in the same, largely relaxed, strain state so that, consequently, any differences in ferroelectric, dielectric, or piezoelectric properties must be ascribed to the differences in the doping of the PZT layers, which couple to polarization in the PMN-PT layers on top.

B. Ferroelectric and piezoelectric properties

The ferroelectric hysteresis (P–E) loops recorded for the different samples are shown in Fig. 2(a). (The loop for the sample without PZT interfacial layer was measured up to ±500 kV/cm and saturates at about ±300 kV/cm.)

It is seen that the polarization hysteresis loops are notably different. First, consider the zero field polarization value $P(0)$, obtained from the extrapolation of the tangent to the high field part of the loop to zero field, which is considered to be a good estimate for saturation polarization (Table II). The $P(0)$ value of the PMN-PT directly on STO/SRO and on Nb-doped PZT is approximately equal (about 19 μC/cm^2) and significantly higher than of the devices on undoped and Fe-doped PZT (about 12 μC/cm^2), see in Table II.

Second, the switching part of the P–E loops is similar for the first group and steeper for the second group [characterized by

TABLE II. Ferroelectric properties of the epitaxial PMN-PT films deposited using no PZT interfacial layer and undoped, respectively, 1% Fe-doped and 1% Nb-doped 25 nm thick PZT interface layers.

Sample	$P(0)$ (μC/cm^2)	$E_{c,av}$ (kV/cm)	E_{sb} (kV/cm)	$\varepsilon_{r,max}$	$(\tan\delta)_{max}$	$\frac{1}{\varepsilon_0}\left(\frac{dP}{dE}\right)_{max}$	$d_{33\mathrm{eff},max}$ (pm/V)
Bulk PMN-PT	43[23]			8200[24]			2800[24]
No-PZT	19.2	26.0	23.6	1862	0.12	5200	52 (−66)
Un-doped	11.5	11.3	−4.9	1970	0.063	3100	65
Fe-PZT	11.9	10.0	−12.0	2800	0.070	4100	73
Nb-PZT	18.8	12.8	−15.3	3455	0.12	7100	67

© Author(s) 2020

the parameter $(dP/dE)/\varepsilon_0$]. The observation that the loops of the undoped and Fe-doped PZT interfacial layer devices are very similar suggests that doping on the A-site hardly affects the polarization of the unit cell. In PMN-PT, the polarization easily rotates under influence of strain and an electric field. The strain states of PMN-PT in these samples are the same, as are seen from the XRD data and lattice parameters; thus, one expects similar polarization behavior, i.e., the same out-of-plane component of the polarization vector (measured $P(0) = P_S \cos\theta(S, E = 0)$ with θ being the angle of the polarization vector, with length P_S with the out-of-plane direction and S being the strain). The much higher polarization of the Nb-doped device, with similar strain as the undoped and Fe-doped devices, hence approximately the same polarization angle, then suggests that the B-site doping enhances the length of the polarization vector P_S. The polarization of that device is similar to that of the no-PZT (S0) device, seems then coincidental, since for that device it is the compressive in-plane strain by the STO/PMN-PT mismatch that increases $\theta(S, E)$, thus $P(0)$.

Another significant difference is the variation in self-bias fields for different devices. The self-bias of the PMN-PT on SRO/STO (sample S0 in Ref. 14) is in the opposite direction as for the devices with a (doped) PZT interfacial layer. In Ref. 14, the self-bias of PMN-PT on SRO/STO was explained by a 16 nm thick strain gradient layer, arising from the compressive strain induced by the SRO/STO that induces an effective field through the flexoelectric effect. The PMN-PT on (doped) PZT is slightly tensile strained, suggesting an opposite flexoelectric effect, hence a (small) negative self-bias, as is observed. {Note that, following the argument in Ref. 14, we think that the (doped) PZT layers are so defective that no strain gradient is present in these PZT layers [since no strong low angle shoulder in the (doped) PZT reflections in the θ–2θ scans is observed].} The difference in self-bias between the devices with undoped and doped PZT must be ascribed to the dopants. The difference in self-bias due to the different valence state of the dopants is small. However, the presence of dopants—irrespective of their valence—seems to enhance the self-bias effect. We speculate that electric dipoles formed by the dopants in the PZT are aligned, causing a small net fixed, upward oriented polarization, creating an additional negative self-bias field. This warrants further experimental study.

The presence of a self-bias field is of great importance, because it affects the performance of devices made from these films. The self-bias field increases the remnant polarization (P_r) in a certain direction (positive or negative remnant polarization) due to the shift of the polarization hysteresis loop.[19]

Similar to the polarization hysteresis loops, the dielectric constant vs field curves are shifted by approximately the same amount as the self-bias field determined from the P–E loops [Fig. 2(b)]. The maximum value of the dielectric constant (Table II) is strongly dependent on the type of interfacial layer, reaching nearly double the maximum value for the Nb-PZT interfacial layer, as compared to the un-doped PZT interfacial layer. At high fields, the dielectric constants become approximately equal, reflecting the nearly parallel slopes of the P–E loops at high fields. Furthermore, the peak splitting of the C–E loops (about 5–10 kV/cm) is much smaller than that of the P–E loop of the same device. In Ref. 20, this was explained by the different responses of domain switching/polarization rotation to the different measurement modes: a fast, constant field change (dE/dt) in the case of the DC-scan for the P–E loop and the low amplitude oscillatory field change in the case of the C–E measurements. This argument was also used to explain the large difference between the maximum relative dielectric constant calculated from the P–E loop (here 3100, 4100, and 7100 for the devices with undoped, Fe-doped, and Nb-doped PZT interface layers, respectively) and the maximum values from the C–E measurements (1970, 2800, and 3455, respectively). There is a large difference in AC domain switching between the PMN-PT on Fe- or Nb-doped PZT and on undoped PZT and without seed layer. The maximum relative dielectric constant determined from C–E measurements of the latter device is only 1862, whereas the maximum slope of the P–E loop of the device without PZT corresponds to a value of 5200, which is of the order of the maximum P–E slope of the PMN-PT/Nb-doped PZT device. This indicates that in the device without a PZT layer, the AC-driven domain wall motion and polarization rotation are much more hampered than for the PMN-PT layers on the doped PZT. The case of PMN-PT on undoped PZT poses an intermediate situation.

Figure 2(c) depicts the loss tangent curves ($\tan\delta - E$) of the four devices. At high fields, the loss is approximately the same for all devices.[20] The large zero-field dielectric constant of the Nb-PZT device is accompanied by a large low field loss of 0.12, whereas the maximum loss of the Fe-PZT device is only 0.07, while the dielectric constant is only 20% less. A similar large difference in loss is found for the device without a PZT interfacial layer and the one with undoped PZT. However, for these films, the dielectric constants are comparable and much lower than for the devices with doped PZT layers. At the moment, we have no explanation for these differences, but the fact that the loss can be manipulated by doping is of interest for applications in which the dielectric loss is important.

Figure 2(d) shows the effective piezoelectric hysteresis ($d_{33eff} - E$) loops of the different devices. The high-field values are approximately equal and in the range of 50–60 pm/V, increasing slightly for lower fields, but overall, the loops are very comparable. These values are strongly reduced compared to the bulk values,[21] due to the clamping of the film to the substrate. The self-bias values observed in the P–E loops are found here again, but the coercive field values of the $d_{33eff} - E$ loops are significantly larger than that of the P–E loops, which is ascribed again to the different measurement modes (AC vs DC) used. The overall similarity of the $d_{33eff} - E$ loops is a reflection of the similar static strain state of the different films, which is not altered by the presence of a thin interfacial layer and is largely determined by the thermal expansion difference between the PMN-PT and the substrate. Since the films are in (nearly) the same strain state, the observed piezoelectric effect of the PMN-PT is also very much the same.

The ferroelectric and dielectric measurements indicate significant differences in the properties between the films with or without (un)doped PZT layers. It was already concluded that structurally there is hardly any difference between these films; thus, the difference in properties must be ascribed to the (non)presence of the additional (doped) PZT interfacial layer.

The first difference is that the coercive field of the device without a PZT layer is more than twice that of the devices with an

© Author(s) 2020

(un)doped PZT interfacial layer. However, there is no clear difference between the coercive fields of the devices with undoped and doped PZT interfacial layers, irrespective of the valence of the dopant. In the model of Gerra *et al.*,[22] a change in interfacial energy between the electrode and the ferroelectric can change the energy barrier for reverse domain nucleation and thus the observed coercive field. Thus, we can conclude that (within this model) the interfacial energy of the SRO/PMN-PT interface is different from that of the SRO/(doped) PZT interface (where we have assumed that the PZT layers are also switchable). Second, it is concluded from the observation that the coercive fields of the devices with (doped) PZT interfacial layers are nearly the same, that the interfacial energy and with that the value of the coercive field do not depend on the valency and lattice position of the dopant but on the type of interface. To our knowledge, there is no literature on the factors that determine this interfacial energy; therefore, we cannot explain more fundamentally what causes the observed differences.

Next to reverse domain nucleation, domain walls must also be able to move to expand the reverse domain size. We observe a significant difference in the maximum steepness of the *P–E* loop of the devices (Table II). Since we concluded that the PMN-PT layers in all devices are the same, the difference in slopes hint toward differences in domain wall pinning properties of the interfacial layers. We do not observe a clear relation between the value of $(dP/dE)_{max}/\varepsilon_0$ and the presence or type of interfacial layer.

The relative dielectric constant ε_r is measured under small signal AC conditions and basically measures the effect of the oscillation of the polarization vector around the equilibrium position in the field bias point. It is seen that for high fields (>100 kV/cm), the dielectric constant is approximately the same for all different devices, which can be explained as follows: at such high fields, the devices are completely poled and the response is solely due to polarization rotation. Since the difference in strain is only small for these devices, one expects that the energy potential around the equilibrium position in the field bias point is approximately the same and, therefore, also the dielectric constant.

$\varepsilon_{r,max}$ is the value found for field values near the switching point of the polarization hysteresis loop. Next to polarization rotation, polarization switching is also important, which implies that the nucleation and growth of domains with a reverse out-of-plane polarization component (and the opposite processes) also contributes and enhances the dielectric response significantly. We observe a significant difference between $\varepsilon_{r,max}$ of devices with doped ($\varepsilon_{r,max} = 2800$ and 3455) and undoped, respectively, no PZT layers ($\varepsilon_{r,max} = 1970$ *and* 1862). As the coercive fields, hence the reverse domain nucleation, are the same for the (un-)doped PZT devices, this leaves a difference in domain wall motion between the doped and undoped PZT devices. Thus, the presence of a charge doped defect layer appears to enhance the domain wall mobility, i.e., easier depinning of the walls. As the effect arises from the doping of the PZT interfacial layer, we think that the pinning sites that cause these differences are inside (for example, dipoles or isolated charged dopants) or near the doped PZT/PMN-PT interface. As there is no significant difference in $\varepsilon_{r,max}$ between the devices with no and an undoped PZT layer, this suggests that the relevant pinning sites are at the SRO/PMN-PT and SRO/PZT interfaces for these devices. The higher $\varepsilon_{r,max}$ values for the doped PZT layer devices indicate a flatter energy landscape for domain wall pinning due to doping. A 1% doping implies that in a given direction, there is an arbitrarily oriented dipole defect in every cube with a side of 4–5 unit cells (this is generally less than the thickness of a non-180° domain wall). We conjecture that the original energy landscape has energetically deeper pinning sites, which are more widely spaced from each other (we expect that the grain boundaries constitute the

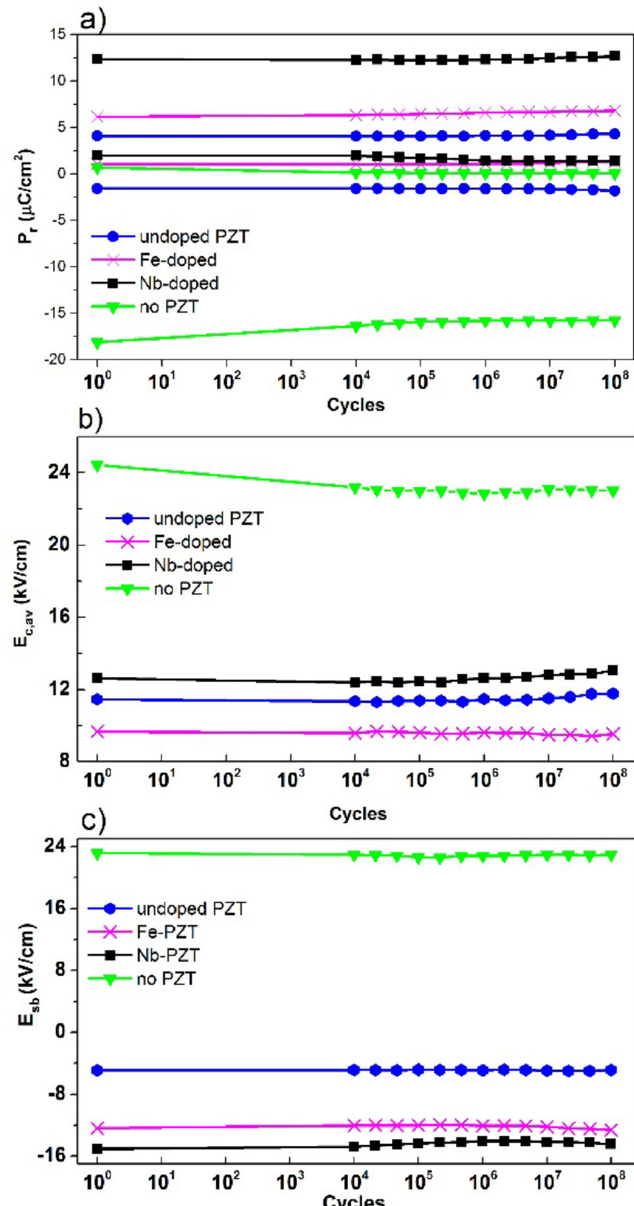

FIG. 3. (a) Remanent polarization, (b) average coercive field, and (c) and self-bias field vs the number of cycles.

© Author(s) 2020

pinning sites, causing locally enhanced strain). The defects introduced by the dopants may relax the local strain and thus reduce the depth of the pinning potential, thus increasing AC susceptibility.

C. Ferroelectric response stability behavior

The stability of the ferroelectric response (aging behavior) of the epitaxial PMN-PT films on doped and undoped PZT interfacial layers was tested by subjecting the devices to a high number (10^8) of switching cycles. Aging behavior in terms of remnant polarization, positive and negative coercive fields [E_{c+} and E_{c-}], a self-bias field [$E_{sb} = (E_{c+} + E_{c-})/2$], and an average coercive field [$E_{c,\,av} = (E_{c+} - E_{c-})/2$] vs number of cycles is shown in Fig. 3. The PMN-PT film on the doped or undoped PZT interfacial layer shows very good ferroelectric response stability against the number of switching cycles. Hardly any changes in the remanent polarization, the coercive field, and the self-bias field are observed for these films up to 10^8 cycles. This reflects the stability of the ferroelectric loop under cycling. The PMN-PT film directly on the SRO/STO shows a slight decrease of remanent polarization and decrease of the width of the hysteresis loop (decreasing $E_{c,av}$), whereas the self-bias is constant.

IV. CONCLUSIONS

Perovskite phase and (001) orientation pure epitaxial PMN-PT films have been prepared on an STO substrate with SRO electrodes. Hard and soft doped PZT interfacial layers as well as undoped PZT interfacial layers were used in between bottom SRO and PMN-PT layers.

Significant differences in ferroelectric and dielectric properties are observed, whereas the piezoelectric properties are very similar. The steepness of the *P–E* loop is reduced by an undoped or a Fe-doped PZT layer, compared to a device with an Nb-doped PZT interfacial layer or without a PZT interface layer. The dielectric constant was nearly doubled by the use of an Nb-doped PZT layer, as compared to an undoped (or no) PZT interface layer. The use of a PZT layer (doped or undoped) slightly enhances the low field effective piezoelectric coefficient. All devices are remarkably stable under up to 10^8 bipolar cycles.

ACKNOWLEDGMENTS

This work was supported by the Engineering Doctorate School of Roma TRE University and by NanoNextNL, a micro- and nanotechnology consortium of the Government of the Netherlands and 130 partners.

DATA AVAILABILITY

The data that support the findings of this study are available from the corresponding author upon reasonable request.

REFERENCES

[1] S. H. Baek, J. Park, D. M. Kim *et al.*, "Giant piezoelectricity on Si for hyperactive MEMS," Science **334**, 958 (2011).

[2] S. E. Park and T. R. Shrout, "Ultrahigh strain and piezoelectric behavior in relaxor based ferroelectric single crystals," J. Appl. Phys. **82**, 1804 (1997).

[3] S. E. Park and T. R. Shrout, "Characteristics of relaxor-based piezoelectric single crystals for ultrasonic transducers," IEEE Trans. Ultrason. Ferroelectr. Freq. Control **44**, 1140 (1997).

[4] D. Damjanovic, *The Science of Hysteresis* (Elsevier, New York, 2005), Vol. 3, p. 337.

[5] B. Jaffe, W. R. Cook, and H. L. Jaffe, *Piezoelectric Ceramics* (Academics Press Inc., New York, 1971).

[6] T. Haccart, D. Remiens, and E. Cattan, "Substitution of Nb doping on the structural, microstructural and electrical properties in PZT films," Thin Solid Films **423**, 235 (2003).

[7] M. D. Nguyen, T. Q. Trinh, M. Dekkers *et al.*, "Effect of dopants on ferroelectric and piezoelectric properties of lead zirconate titanate thin films on Si substrates," Ceram. Int. **40**, 1013 (2014).

[8] Z.-X. Zhu, C. Ruangchalermwong, and J.-F. Li, "Thickness and Nb doping effects on ferro and piezoelectric properties of highly axis oriented Nb-doped Pb$(Zr_{0.3}Ti_{0.7})O_3$ films," J. Appl. Phys. **104**, 054107 (2008).

[9] C. Ruangchalermwong, J.-F. Li, Z.-X. Zhu *et al.*, "Enhanced ferro- and piezoelectric properties in (100)-textured Nb-doped $Pb(Zr_xTi_{1-x})O_3$ films with compositions at morphotropic phase boundary," Thin Solid Films **517**, 6599 (2009).

[10] S. B. Majumder, B. Roy, R. S. Katiyar, and S. B. Krupanidhi, "Effect of acceptor and donor dopants on polarization components of lead zirconate titanate thin films," Appl. Phys. Lett. **79**, 239 (2001).

[11] W. Bai, X. J. Meng, T. Lin *et al.*, "Effect of Fe-doping concentration on microstructure, electrical, and magnetic properties of $Pb(Zr_{0.5}Ti_{0.5})O_3$ thin films prepared by chemical solution deposition," J. Appl. Phys. **106**, 124908 (2009).

[12] M. Dawber and J. F. Scott, "A model for fatigue in ferroelectric perovskite thin films," Appl. Phys. Lett. **76**, 1060 (2000).

[13] W. L. Warren, G. E. Pike, K. Vanheusden *et al.*, "Defect dipole alignment and tetragonal strain in ferroelectrics," J. Appl. Phys. **79**, 9250 (1996).

[14] M. Boota, E. P. Houwman, M. Dekkers *et al.*, "Epitaxial $Pb(Mg_{1/3}Nb_{2/3})O_3$-$PbTiO_3$ (67/33) thin films with large tunable self-bias field controlled by a $PbZr_{1-x}Ti_xO_3$ interfacial layer," Appl. Phys. Lett. **104**, 182909 (2014).

[15] S. A. Yang, S. Y. Cho, J. S. Lim, and S. D. Bu, "Distribution of pyrochlore phase in $Pb(Mg_{1/3}Nb_{2/3})O_3$-$PbTiO_3$ films and suppression with a Pb$(Zr_{0.52}Ti_{0.48})O_3$ interfacial layer," Thin Solid Films **520**, 7071 (2012).

[16] G. Koster, B. L. Kropman, G. J. H. M. Rijnders *et al.*, "Quasi-ideal strontium titanate crystal surfaces through formation of strontium hydroxide," Appl. Phys. Lett. **73**, 2920 (1998).

[17] M. Boota, E. P. Houwman, M. D. Nguyen *et al.*, "Effect of fabrication conditions on phase formation and properties of epitaxial $(PbMg_{1/3}Nb_{2/3}O_3)_{0.67}$-$(PbTiO_3)_{0.33}$ thin films on (001) $SrTiO_3$," AIP Adv. **6**, 055303 (2016).

[18] G. A. Rossetti, A. G. Khachaturyan, G. Akcay, and Y. Ni, "Ferroelectric solid solutions with morphotropic boundaries: Vanishing polarization anisotropy, adaptive, polar glass, and two-phase states," J. Appl. Phys. **103**, 114113 (2008); Z. Zhang, J.-H. Park, and S. Trolier-McKinstry, *MRS Proceedings 596 Ferroelectric Thin Films VIII*, edited by R. W. Schwartz, P. C. McIntyre, Y. Miyasaka, S. R. Summerfelt, and D. Wouters (Materials Research Society, Warrendale, PA, 2000), p. 73.

[19] M. Boota, E. P. Houwman, M. Dekkers *et al.*, "Properties of epitaxial, (001)- and (110)-oriented $(PbMg_{1/3}Nb_{2/3}O_3)_{2/3}$-$(PbTiO_3)_{1/3}$ films on silicon described by polarization rotation," Sci. Technol. Adv. Mat. **17**, 45 (2016).

[20] The opening of the loop of the "no-PZT" device at the maximum and minimum field values is because this loop was measured up to ±400 kV/cm (where the loop is closed) and truncated to fit in this figure.

[21] F. Li, L. Jin, D. Wang, and S. Zhang, "Electrostrictive effect in $Pb(Mg_{1/3}Nb_{2/3})O_3$-x$PbTiO_3$ crystals," Appl. Phys. Lett. **102**, 152910 (2013).

[22] G. Gerra, A. K. Tagantsev, and N. Setter, "Surface-stimulated nucleation of reverse domains in ferroelectrics," Phys. Rev. Lett. **94**, 107602 (2005).

[23] R. Zhang, B. Jiang, and W. Cao, "Elastic, piezoelectric, and dielectric properties of multidomain $0.67Pb(Mg_{1/3}Nb_{2/3})O_3$–$0.33PbTiO_3$ single crystals," J. Appl. Phys. **90**, 3471 (2001).

[24] S. Zhang and F. Li, "High performance ferroelectric relaxor-$PbTiO_3$ single crystals: Status and perspective," J. Appl. Phys. **111**, 031301 (2012).

© Author(s) 2020